IEEE Access
Multidisciplinary | Rapid Review | Open Access Journal

Received 4 September 2023, accepted 2 October 2023, date of publication 12 October 2023, date of current version 18 October 2023.

Digital Object Identifier 10.1109/ACCESS.2023.3324195

RESEARCH ARTICLE

Scalable Acoustical Frequency Tagging Coherent Beam Combining Based on Digital Signal Processing

PAWEL R. KACZMAREK, ALEKSANDER GLUSZEK, AND ARKADIUSZ HUDZIKOWSKI
Laser and Fiber Electronics Group, Wroclaw University of Science and Technology, 50-370 Wroclaw, Poland

Corresponding author: Pawel R. Kaczmarek (pawel.kaczmarek@pwr.edu.pl)

This work was supported in part by the National Centre for Research and Development of Poland in the Framework of Strategic Program under Grant DOB-1-6/1/PS/2014.

ABSTRACT We present the module of booster amplifier for coherent beam combining Master Oscillator Power Amplifier (MOPA) system to operate with a narrow-linewidth seed laser. The goal was to achieve a highly modular system, manifested in the ease of changing the number of Coherent Beam Combining (CBC) channels. It uses a frequency tagging phase control scheme performed at acoustical frequencies, enabling a simple piezo fiber stretcher as actuating and tagging element and a cheap microcontroller to perform all the signal processing. The four-channel CBC system with the proposed booster module was built to verify our assumptions and the whole system's performance.

INDEX TERMS Coherent beam combining, frequency tagging, MOPA, piezo phase shifter.

I. INTRODUCTION

Stimulated Brillouin Scattering (SBS) is the main limiting factor for a high power density narrow-line signal propagating in the optical fiber [1]. The SBS threshold for a particular fiber system and given linewidth can be increased typically by the three most common approaches. The simplest method is to use fibers with a larger core and mode field diameter, called Large Mode Area (LMA) fibers, thus lower power density for given optical power propagating in the fiber [2], [3]. The other methods are based on the fact that Brillouin frequency shift is temperature [1] and stress [4], [5] dependent. Hence, introducing the fiber's temperature or stress gradient increases the fiber system's SBS threshold. The last possibility is to use a broader seed laser spectrum or artificially broaden its spectra by modulation [6], [7]. However, it is not applicable for systems where narrow linewidth is a crucial parameter.

Nevertheless, increasing amplifier output power can meet hard limits, and the whole system's redesign may be required. For example, above some level of the fiber system's output power, all the ways to raise an SBS threshold are insufficient. In that particular case, an approach needs to be changed. Instead of increasing the single fiber amplifier's output power, a system with parallel amplifiers can be used. Such a system output power can be close to the sum of powers of each amplifier module working below its SBS threshold [8]. Each amplifier's phase shift must be controlled and match other channel phases to maintain the high efficiency of adding all parallel output beams [9]. This method is the so-called Coherent Beam Combining (CBC), typically used with high power systems [10], [11], [12] or high peak power ultrafast lasers [13], [14].

The associate editor coordinating the review of this manuscript and approving it for publication was Norbert Herencsar.

II. THE PROBLEM DEFINITION

One of the main goals of our work is to develop a simple, scalable, and cost-effective system for amplifying a narrow linewidth laser source. Our seed laser was settled to be a Diode-Pumped Solid-State Laser (DPSSL) developed in our group with narrow linewidth $\Delta\nu < 100$ kHz [15]. Reaching tens of watts of output power implies the utilization of Master Oscillator Power Amplifier (MOPA) configuration. The output power of such a system is limited by the SBS threshold of the last amplifying stage in the case of a narrow linewidth source. Since the simplicity of the amplifier was our aim, we have decided to use the most straightforward solution [2] in our setup: dedicated for such applications LMA fibers. It was commercially available ytterbium-doped double-clad fiber PLMA-YDF-10/125-HI-8 as a gain medium and

© 2023 The Authors. This work is licensed under a Creative Commons Attribution-NonCommercial-NoDerivatives 4.0 License.
For more information, see https://creativecommons.org/licenses/by-nc-nd/4.0/

matched passive LMA fiber as an output fiber. The chosen way allows us to reach the Ytterbium Doped Fiber Amplifier (YDFA) output power of 10 W relatively easily, which is very hard to get in standard single-mode fiber for the wavelength. In figure 1, a setup of amplifier and comparison of two YDFAs based on standard and LMA fibers is presented.

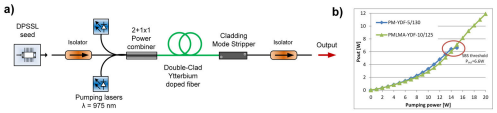

FIGURE 1. Ytterbium-doped fiber amplifier: a) configuration, b) output characteristics for standard and LMA active fibers.

In both cases, an amplifier was pumped by two 10 W pumping lasers. The 976 nm pumping wavelength was chosen to obtain the shortest active fiber length in the amplifier, which is essential regarding the SBS threshold. Output fiber length should also be minimized, which forces usage of a co-propagating pumping scheme. As a seed laser, a single-mode narrow line DPSSL was used. One can quickly notice a saturation of above 6 W of output power for the standard single-mode fiber, which is caused by exceeding the system's SBS threshold. LMA fiber amplifier does not show any SBS sign, up to maximum pumping power of 20 W. Since the mode field area for LMA fiber is approximately four times higher, one can roughly estimate the SBS threshold to be higher than 20W. It has proved that chosen straightforward booster amplifier configuration is a proper way for a single module fiber amplifier to reach 10 W of output power. It gives a safe margin for using even DPSSL with twice the narrower linewidth to the seed we used. To avoid the SBS limit for the MOPA system and remain with the last stage simple configuration, a CBC approach was used with a phase synchronization of the parallel output beams. Unlike the high-power or ultrashort pulse systems, there is no need to align optical pathways accurately in each channel for narrow-line lasers. The coherence length is large enough for the differences, even as high as tens of meters or so. The only thing that needs to be done is to have a control circuit able to change each amplifier output phase fast enough to keep all channel phase relations constant. The main reason for the amplifier's output phase instability is the change of its optical length. This phenomenon can even control the output phase without additional phase modulators necessary [16]. For designing a phase control system, there is the necessity to determine what typical phase shift changes speed is.

We measured phase fluctuations of the amplifier model described above in a standard Mach-Zehnder interferometer. The setup for the measurement is depicted in figure 2. The amplifier's output beam was collected by a sample fiber and then interfered in the fiber coupler with the reference beam. On the scope, interference fringes were observed due to phase changes in the amplifier's arm of the interferometer.

Since an amplifier is made of optical fiber, optical length changes can be induced by mechanical stresses, temperature changes, or the amplifier's pumping power [17].

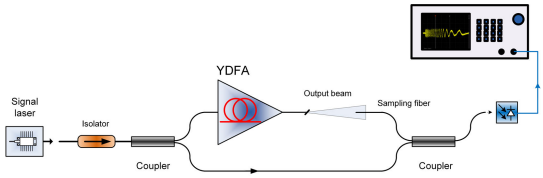

FIGURE 2. The Mach-Zehnder interferometer setup for measuring the YDFA's output phase fluctuations.

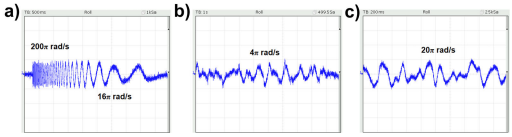

FIGURE 3. The signals recorded when testing phase fluctuations at the amplifier output. a) signal when pump current is stepped on, b) signal when the environment is unstable, c) signal when the pump current is chaotically modulated by 0.5 A.

Figure 3 shows a couple of examples of signals recorded in typical scenarios. Amplifier pumping power changes induce the fastest and most significant phase changes. It is visible in figure 3a recorded after turning on the amplifier pumping power from 0 up to half of the maximum power. After the pumping power step, a high density of fringes means phase change as fast as 0.2 π rad/ms. However, two seconds after, it decreases to the value of 16 π rad/s.

Phase fluctuations for environmentally induced fiber length changes are much slower, with a typical value of 4 π rad/s (figure 3b). Faster modulations were made by pumping power rapid change. In figure 3c, chaotic variation of pumping power with an amplitude of 1 W was depicted. Such pumping power changes do not produce phase modulation faster than 20 π rad/s. These results of measurements allowed us to estimate requirements for the phase controlling circuit bandwidth. We have settled the servo loop bandwidth to 1 kHz for all controlling circuits, which will be several times faster than observed changes.

III. PHASE SYNCHRONIZATION CONCEPT

The small phase control bandwidth required for the system allows using of slow fiber phase shifters. On the other hand, typical frequency tagging systems typically utilize fast Electro-Optical Modulators (EOM) to tag each channel with an individual Radio Frequency (RF) [11], [18], [19], [20], [21]. It requires sophisticated RF electronics to make the whole control circuit, and in the case of the narrow-linewidth laser as a seed, it can significantly broaden the laser spectra. Since the phase control bandwidth required is not high, we have decided to apply slow phase modulators for frequency tagging and phase actuation. Our choice was to make a fiber stretcher based on the piezo tube. It was proven that this kind of phase modulator has enough bandwidth to efficiently control phase in a multi-dithering CBC system [22], [23]. The fiber stretcher was made using a piezoelectric ceramic tube of diameters outer 38 mm and 31 mm inner with a height of 25 mm. The external diameter is big enough not to introduce significant bending losses for the single-mode

PM980 fiber. The piezo tube's catalog resonance frequency was 25 kHz, which allows operating as a linear phase shifter with a bandwidth of almost 10 kHz. Seventy turns of HI980 Polarization Maintaining (PM) bend-insensitive fiber were wound up on the tube. A device's photo is shown in figure 4a and its frequency amplitude response in figure 4b. The modulation coefficient is high due to the high number of fiber turns on the tube. Such a high coefficient allows having an increased depth of the phase modulation with relatively low phase controlling signal amplitudes.

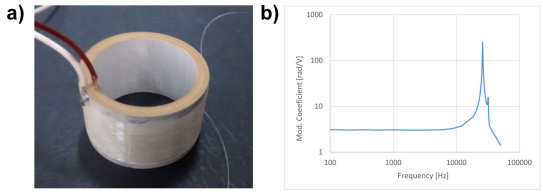

FIGURE 4. Piezotube fiber stretcher. a) a photo of the device, b) modulation coefficient frequency characteristics.

The phase modulator has a high Q resonance at a frequency of 26 kHz and a flat response characteristic of 10 kHz with a modulation coefficient of 0.9 π rad/V. With such a phase modulator, we were able to develop and design the whole system concept. The most common method for synchronizing all the phases in CBC systems is a Stochastic Parallel Gradient Descent (SPGD) algorithm. The main advantage is the low bandwidth required for phase control and actuation circuits, including the phase modulators [24]. The method requires a single unit, shared by all the channels, and performing phase shift control for all the channels and synchronizing them [8], [25]. As the main disadvantage, one can consider the system's scalability since the time to convergence strongly depends on the number of synchronized channels [26]. We assume high modularity of the designed system, which enables easy system scaling by channel addition. This requirement practically eliminates an SPGD approach to making such a system (central synchronizing unit). An ideal modular system should have as few elements common for all the channels as possible. The frequency tagging CBC method allows the system's high modularity since each phase control channel can be completely independent of the others. The only common point for the system is, in this case, a photodetector and seed source. A typical frequency tagging system uses RF EOM modulators for marking each channel with an individual frequency [27]. Such a requirement is essential if the system deals with fast phase changes. It requires wide bandwidth of the phase control loop. For slow phase changes, slow-speed phase modulators can be applied in such systems as an actuator for aligning the phase of each channel. RF frequency tagging requires using RF electronics and can broaden the laser line in narrow linewidth laser systems. However, knowing the bandwidth necessary for the phase control loop, one can see that system's channel spacing can be low for slow phase changes. It allows considering a frequency tagging system, operating fully with the PZT tube phase modulators. It is presented in [23] and [28]. This approach can significantly simplify the phase control loop electronics and enable the use of cheap digital signal processing units based on commonly available microcontrollers. Especially the latest solution is desirable regarding the flexibility of the system and its cost-effectiveness.

The frequency tagging system principles of operation are as follows. It maximizes the optical signal detected by a single photodetector placed in the far-field pattern's central point (for tiled aperture systems). Each channel's contribution to the signal is determined by small phase modulation with a unique frequency. Though systems using the same frequency for all the channels are reported, they require a central unit synchronizing the whole system [29]. Extraction of the phase control signal is done by a lock-in amplifier scheme allowing for channel-specific signal distinction. To optimize the phase control characteristic, a PID controller has to be applied. A single phase modulator can be used as an actuator for phase correction and tagging tasks since all the signals are in the same low-frequency range. In figure 5, a block diagram for the phase control loop is shown. Almost all signal processing, tagging and actuating, for our setup are done in the digital domain.

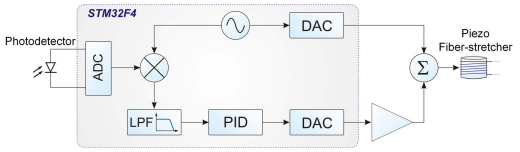

FIGURE 5. Block diagram of digital signal processing CBC system.

The main computation cost for the phase control loop algorithm is Low Pass Filter (LPF) calculation. A choice of the popular microcontroller based on the ARM core was taken to meet the task. STM32F4 family microcontroller, with Floating Point Unit (FPU) and dedicated Digital Signal Processing (DSP) instructions set to perform one step of the whole frequency tagging algorithm with a frequency over 200 kHz, was ideal for this solution. It limits marking frequency to 100 kHz, which was enough regarding the phase modulator bandwidth. A simple setup shown in figure 6 was built to check all design requirements. The results of such simulated operation of a two-channel CBC system are presented in figure 7. It is a simple Mach-Zehnder interferometer with two phase modulators placed in the one of its arms. One was dedicated to the phase fluctuations simulation driven by the signal generator marked by a red signal in figures 6 and 7. The second one was an actuator for the evaluation board-based version of the proposed frequency tagging phase control loop denoted as blue signals. At the interferometer output, two photodetectors were attached. The green one was a signal used for the frequency tagging phase control system, which drives the actuator to maximize its value. The second photodetector (magenta color) is complementary, keeping a minimum of the optical power under system operation.

While the first modulator changes the phase according to the generator's signal, the phase control loop maximizes one

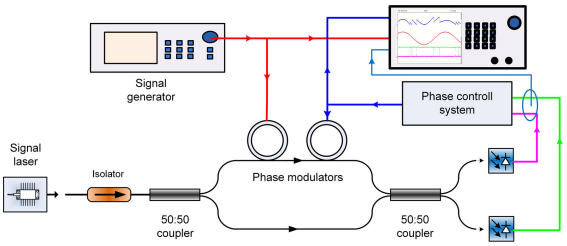

FIGURE 6. The setup for the model of simple two-channel CBC system for validation of acoustical frequency tagging system.

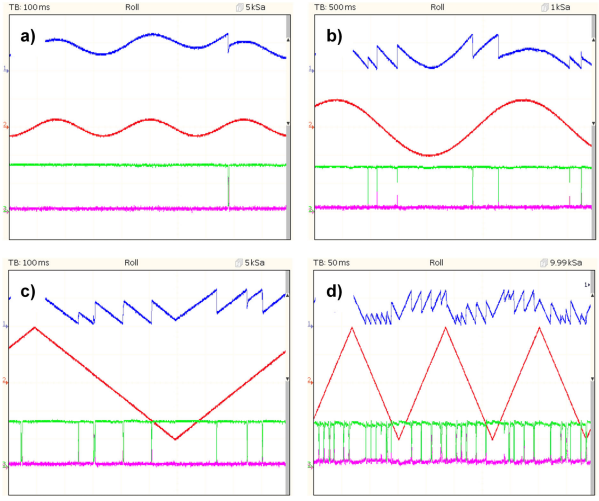

FIGURE 7. Two-channel acoustical frequency tagging CBC system performance: a) synchronization on - simulation of phase changes in the "holding" range of the system, b) phase modulation by 9π rad, c) fast modulation 36π rad/s, d) high-speed modulation 216 π rad/s.

of the photodetector signals, minimizing the phase difference between both arms. For small phase modulation, an actuating signal follows the signal driving simulating modulator. The digitally controlled synchronization loop's advantage appears when the actuating voltage reaches the limit for its output circuits. Implementation of the step in actuator controlling voltage gives the possibility to change the phase strictly by a 2π rad. One can notice such phase jumps in actuating and photodetector signals (figure 7a). During a jump, the setup is temporarily out of synchronization state, which can be seen as a sudden drop of photodetector voltage. After a while, de-pendant on the LPF bandwidth, PID ratios, and the actuator response time, the system goes back to the in-synchro state. For evaluation purposes, cases with various depths and speeds of the phase modulation were tested. For the instances shown in fig. 7b-d, the phase change is more significant than the loop's lock range (determined by a range of voltages driving the actuating phase modulator). CBC controller's performance, consistent with the speed of phase changes for the values measured in the YDFA model, was sufficient. Even for the phase changes as fast as 36 π rad/s, a photodetector trace and general performance of the loop were similar to the slow phase changes performance (fig 7c and b, respectively). The only difference was the number of phase jumps visible in the signal. Just during the highest phase change speed recorded for turning on the ytterbium amplifier (fig 3a. and fig 7d.), exceeding 0.2 π rad/ms, a visible drop in the synchronization quality was observed. Between the phase jumps, the photodetector signal was not maximized, and it was fluctuating. It is still a kind of synchronization since the photodetector in a loop has a significantly higher level than the second one but with lower efficiency caused by phase matching error.

IV. THE ACTIVELY PHASE-CONTROLLED BOOSTER AMPLIFIER MODULE

After testing the system stability, an entire amplifier module designed for parallel multi-channel, frequency tagging CBC was finally formed. The amplifier module consists of an input phase modulator, optical state detection circuits, and an output power amplifier. An STM microcontroller controlled the whole module. It was responsible for: controlling and monitoring the temperature of pumping lasers (two 10W diodes), detection of optical power levels in the system, general temperature monitoring of critical components, user interface (display and keyboard), and most important - implementation of the digital phase stabilization algorithm by the frequency tagging method. The schematic of the amplifier module is shown in figure 8. The optical output power of the module was 10 W, with 200 mW of minimum input power.

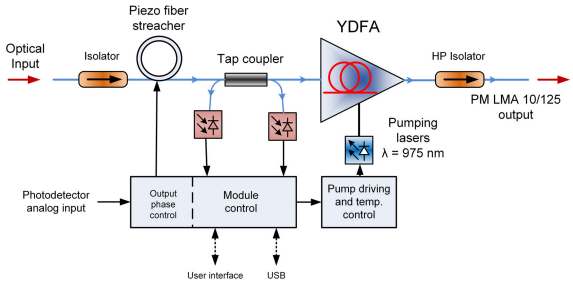

FIGURE 8. Block diagram of universal amplifier module for scalable CBC systems.

The developed amplifier module block diagram was optimized to be as simple as possible. It has an optical signal input, an optical signal output, and an electrical photodetector signal input. Nothing else was needed for its proper operation in the CBC circuit. However, fabricating the module, one additional factor had to be considered. The spectral width of the seed laser was a crucial parameter. It determines the precision of the fiber length matching needed between all used amplifier modules. Therefore, any differences in optical paths should be significantly shorter than the coherence length of the seeding light. Otherwise, a significant decrease of CBC efficiency will occur manifested by decreasing of the far-field pattern reduced contrast. However, in the case of narrow-line DPSSL seed, even a couple of meter imbalances between channels do not deteriorate the CBC system performance.

The software sets individual tagging frequency, taking values from 4 kHz to 60 kHz range with exception for the modulator resonance neighborhood. The lowpass filter in the circuit was designed for 1 kHz, which forces at least a 2 kHz distance between the channels to avoid the crosstalk.

The tagging frequencies harmonics overlapping with the basebands of the other channels also have to be considered during the channel operating frequencies selection. Since our system can only work in such a high modulation bandwidth and four channels, there was no need to use the modified multi-dithering technique with its limits [28]. However, increasing the number of channels may require applying it to maintain the required phase control bandwidth.

V. RESULTS AND DISCUSSION

The four-channel system in classical MOPA configuration was built to verify the concept of the universal amplifier for CBC. As a seed laser, a narrow line single frequency DPSSL pigtailed into PM single-mode fiber was used. The next stage was a typical YDFA based on standard single-mode PM fiber. Its output power was higher than 1 W, driving four parallel power stages described above. The output of the CBC system was built in the tiled aperture scheme. We have decided to use this setup instead of filed aperture scheme regarding the system's free space part's simplicity and scalability. The setup is presented in figure 9.

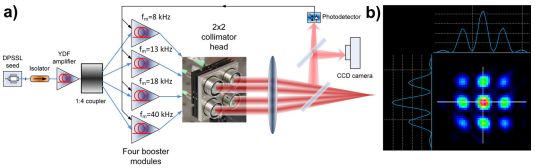

FIGURE 9. a) Four-channel tiled aperture CBC system, b) far-field pattern.

Each channel has an individual tagging frequency, programmed according to the rules mentioned above. According to the phase shifter frequency response, the tagging frequency has to be chosen at some distance from the resonant frequency. It can be either below or above the resonance. Though the fiber stretcher's amplitude and phase response are not linear, the phase control loop works well even for as high tagging frequencies as 60 kHz. Since we decided to choose a tiled aperture CBC scheme, a long focal length lens was used to form the far-field pattern. The small amount of output beam was outcoupled to the CCD camera and sampling photodetector. Since it was only proof of concept work, we did not maximize far-field CBC spatial efficiency. Therefore, the Fill Factor (FF) for our head was not fully optimal, especially the 2 × 2 symmetrical configuration [30], [31]. Figure 9b presents a far-field intensity pattern for the setup with all 4 CBC amplifiers synchronized. The pattern was stable with the control loop closed. Sometimes a tiny trembling, connected with phase jumps, was visible. The fringe contrast was high, exceeding 95%, proving the system's usability.

A fiber pigtailed photodiode takes the input signal for phase synchronization from the middle of the far-field pattern. Since the mode field diameter of the used fiber was significantly smaller than the central lob of the pattern, it has acted as a pinhole, allowing a good quality signal for the tiled aperture CBC system.

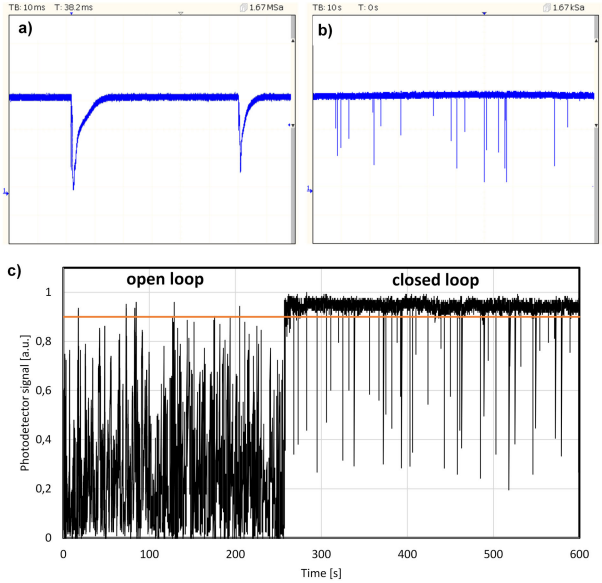

FIGURE 10. A photodetector signals recorded during four-channel CBC system operation; a) 100 ms time span, b) 100 s time span, c) long time scale with open control loop (left) and closed loop (right) with marked 0.9 level (red).

In figure 10, a set of photodetector signals recorded under the 2 × 2 CBC system operation is presented. The whole system works to maximize the photodetector signal and tries to find a ''common phase''. It is a so-called self-synchronous mode [32]. However, it can also work with one of the channels without active phase stabilization and act as a reference channel which is called self-referenced mode. For stable environmental conditions, only occasional phase jumps were observed. The recovery after phase jump typically takes less than 5 ms with a maximum (fig. 10a.) of 12 ms. Figure 10bc presents a long-timescale signal. In any case, there were no more than 50 phase jumps for such a long period. We directed the air conditioning blow directly to the optical table with our setup to simulate the volatile environment. It has also introduced vibrations and movement of all loose fibers on the table. During increased phase fluctuations in all the channels, the average frequency of the phase jumps was increased and reached approximately 2 Hz. Even though in the worst-case scenario, which assumes 10 ms jumps, over 98% of the system operation time keeps stable power on all four channels phase locking. In addition to phase jumps temporarily throwing the system out of balance, it is also another essential factor informing how accurately the system stabilizes the phases. This measure is known as residual phase control error. Figure 10c shows the time domain photodetector signal observed with phase control off and then on. Without phase control, the signal randomly oscillates between 0 and maximum. When phase control is enabled, the photodetector signal has a value above 0.9 maximum most of the time, exept phase jumps. It means the residual phase control error is slightly better than $\lambda/20$ [23].

TABLE 1. Different CBC systems comparison.

Config	Scalability	Cost effectiveness	Line widening	Ref.
	Modularity	RF electronics		
Acoustical frequency tagging	limited excellent	high none	small to none	this work
Classical SPGD	moderate none	moderate none	none	[8], [12], [25], [26]
Classical LOCSET	very good possible	low yes	yes	[10], [11], [18]
Differential phase control	low none	low yes	yes	[16]
Heterodyne detection	low, costly none	poor yes a lot	none	[17]
PRBS modulated LOCSET	good possible	low yes	extreme	[20]
Multidithering	limited possible	low yes	yes	[21]
Two PZT multidithering	potentially good none	moderate none	small	[23]
M-LOCSET	poor possible	high none	small	[28]
Single frequency dithering	poor none	low yes	yes	[29]
Interferometric hill climb	none none	low none	none	[31]

VI. CONCLUSION

Table 1 shows a comparison of selected CBC systems presented to date. The comparison is based on three main aspects. The first is the scalability of the system and its modularity. The scalability issue is well described in the literature and needs no further explanation. Modularity, however, is the ease of adding more CBC channels without modifying the rest of the system. As a rule, CBC systems based on the SPGD method or derivatives are not modular, requiring a single controller common to all channels. On the other hand, systems based on frequency tagging, like presented in this works, are scalable. To present moment, however, no publication has raised this advantage directly. We have built our system with this approach from the beginning. Each CBC channel is entirely independent of the others, and the only common element in the phase synchronization system is the single photodetector.

The second major differentiating factor between the CBC systems described in the literature and ours is their cost-effectiveness. It is related with two main components. The type of phase modulators used - systems operating at high frequencies require expensive fiber-pigtailed electro-optical modulators and the need for RF electronics. Here, systems operating at low frequencies (acoustic or low ultrasound) are the most cost-effective. They allow low-cost piezoelectric fiber-stretcher phase modulators and low-cost analog electronics, because most of the signal processing can be done digitally with standard microcontrollers.

The last criterion is the chosen technique's suitability for spectrally narrow light sources. It is closely related to the modulation bandwidth needed for phase stabilization leading to laser linewidth broadening.

For the cases where modularity and scalability go together with narrow spectral linewidth requirements, both SPGD methods and classical RF frequency tagging systems could be troublesome. We have proposed a novel, cost-effective approach to make an easily scalable acoustical frequency tagging CBC modular system. Our module of YDF amplifier for CBC has been tested in the 2×2 CBC setup, proving the design assumptions. The results are promising, and there is a field for further optimization. Especially the recovery time after phase jump could be shortened, by the signal processing parameters optimization. Channel spacing and its connection to the LPF bandwidth, regarding the system scalability, can also be improved in the future by applying the modified multi-dithering technique proposed in [28].

REFERENCES

[1] M. Hildebrandt, S. Buesche, P. Wessels, M. Frede, and D. Kracht, "Brillouin scattering spectra in high-power singlefrequency ytterbium doped fiber amplifiers," *Opt. Exp.*, vol. 16, no. 20, pp. 15970–15979, Sep. 2008, doi: 10.1364/OE.16.015970.

[2] A. Kobyakov, M. Sauer, and D. Chowdhury, "Stimulated Brillouin scattering in optical fibers," *Adv. Opt. Photon.*, vol. 2, no. 1, p. 1, Mar. 2010, doi: 10.1364/AOP.2.000001.

[3] Y. Jeong, J. Nilsson, J. K. Sahu, D. N. Payne, R. Horley, L. M. B. Hickey, and P. W. Turner, "Power scaling of single-frequency ytterbium-doped fiber master-oscillator power-amplifier sources up to 500 W," *IEEE J. Sel. Topics Quantum Electron.*, vol. 13, no. 3, pp. 546–551, May/Jun. 2007, doi: 10.1109/JSTQE.2007.896639.

[4] J. M. C. Boggio, J. D. Marconi, and H. L. Fragnito, "Experimental and numerical investigation of the SBS-threshold increase in an optical fiber by applying strain distributions," *J. Lightw. Technol.*, vol. 23, no. 11, pp. 3808–3814, Nov. 2005, doi: 10.1109/JLT.2005.856226.

[5] L. Zhang, S. Cui, C. Liu, J. Zhou, and Y. Feng, "170 W, single-frequency, single-mode, linearly-polarized, Yb-doped all-fiber amplifier," *Opt. Exp.*, vol. 21, no. 5, p. 5456, Mar. 2013, doi: 10.1364/OE.21.005456.

[6] B. Anderson, A. Flores, R. Holten, and I. Dajani, "Comparison of phase modulation schemes for coherently combined fiber amplifiers," *Opt. Exp.*, vol. 23, no. 21, p. 27046, Oct. 2015, doi: 10.1364/OE.23.027046.

[7] M. W. Hyde, G. A. Tyler, and C. R. Garcia, "Target-in-the-loop phasing of a fiber laser array fed by a linewidth-broadened master oscillator," *Proc. SPIE*, vol. 10192, May 2017, Art. no. 101920K, doi: 10.1117/12.2257581.

[8] P. Zhou, Z. Liu, X. Wang, Y. Ma, H. Ma, and X. Xu, "Coherent beam combining of two fiber amplifiers using stochastic parallel gradient descent algorithm," *Opt. Laser Technol.*, vol. 41, no. 7, pp. 853–856, Oct. 2009, doi: 10.1016/j.optlastec.2009.03.002.

[9] T. Y. Fan, "Laser beam combining for high-power, high-radiance sources," *IEEE J. Sel. Topics Quantum Electron.*, vol. 11, no. 3, pp. 567–577, May 2005.

[10] T. M. Shay, J. T. Baker, A. D. Sanchez, C. A. Robin, C. L. Vergien, C. Zeringue, D. Gallant, C. A. Lu, B. Pulford, T. J. Bronder, and A. Lucero, "High-power phase locking of a fiber amplifier array," *Proc. SPIE*, vol. 7195, Feb. 2009, Art. no. 71951M, doi: 10.1117/12.809416.

[11] S. J. McNaught, P. A. Thielen, L. N. Adams, J. G. Ho, A. M. Johnson, J. P. Machan, J. E. Rothenberg, C.-C. Shih, D. M. Shimabukuro, M. P. Wacks, M. E. Weber, and G. D. Goodno, "Scalable coherent combining of kilowatt fiber amplifiers into a 2.4-kW beam," *IEEE J. Sel. Topics Quantum Electron.*, vol. 20, no. 5, pp. 174–181, Sep. 2014, doi: 10.1109/JSTQE.2013.2296771.

[12] P. Ma, H. Chang, Y. Ma, R. Su, Y. Qi, J. Wu, C. Li, J. Long, W. Lai, Q. Chang, T. Hou, P. Zhou, and J. Zhou, "7.1 kW coherent beam combining system based on a seven-channel fiber amplifier array," *Opt. Laser Technol.*, vol. 140, Aug. 2021, Art. no. 107016, doi: 10.1016/j.optlastec.2021.107016.
[13] A. Klenke, E. Seise, J. Limpert, and A. Tünnermann, "Basic considerations on coherent combining of ultrashort laser pulses," *Opt. Exp.*, vol. 19, no. 25, p. 25379, Dec. 2011, doi: 10.1364/OE.19.025379.
[14] M. Hanna, F. Guichard, Y. Zaouter, D. N. Papadopoulos, F. Druon, and P. Georges, "Coherent combination of ultrafast fiber amplifiers," *J. Phys. B, At., Mol. Opt. Phys.*, vol. 49, no. 6, Mar. 2016, Art. no. 062004, doi: 10.1088/0953-4075/49/6/062004.
[15] G. Dudzik, J. Sotor, K. Krzempek, G. Sobon, and K. M. Abramski, "Single-frequency, fully integrated, miniature DPSS laser based on monolithic resonator," *Proc. SPIE*, vol. 8959, Feb. 2014, Art. no. 89591F, doi: 10.1117/12.2038518.
[16] H. Tünnermann, Y. Feng, J. Neumann, D. Kracht, and P. Weßels, "All-fiber coherent beam combining with phase stabilization via differential pump power control," *Opt. Lett.*, vol. 37, no. 7, p. 1202, Apr. 2012, doi: 10.1364/OL.37.001202.
[17] S. J. Augst, T. Y. Fan, and A. Sanchez, "Coherent beam combining and phase noise measurements of ytterbium fiber amplifiers," *Opt. Lett.*, vol. 29, no. 5, p. 474, Mar. 2004, doi: 10.1364/OL.29.000474.
[18] T. M. Shay, V. Benham, J. T. Baker, B. Ward, A. D. Sanchez, M. A. Culpepper, D. Pilkington, J. Spring, D. J. Nelson, and C. A. Lu, "First experimental demonstration of self-synchronous phase locking of an optical array," *Opt. Exp.*, vol. 14, no. 25, p. 12015, Dec. 2006, doi: 10.1364/OE.14.012015.
[19] M. W. Hyde and G. A. Tyler, "Temporal coherence effects on target-based phasing of laser arrays," *J. Opt. Soc. Amer. A, Opt. Image Sci.*, vol. 33, no. 10, p. 1931, Oct. 2016, doi: 10.1364/JOSAA.33.001931.
[20] A. Flores, I. Dajani, R. Holten, T. Ehrenreich, and B. Anderson, "Multi-kilowatt diffractive coherent combining of pseudorandom-modulated fiber amplifiers," *Opt. Eng.*, vol. 55, no. 9, Sep. 2016, Art. no. 096101, doi: 10.1117/1.OE.55.9.096101.
[21] L. Liu, D. N. Loizos, M. A. Vorontsov, P. P. Sotiriadis, and G. Cauwenberghs, "Coherent combining of multiple beams with multi-dithering technique: 100 KHz closed-loop compensation demonstration," presented at *Opt. Eng. Appl.*, San Diego, CA, USA, Sep. 2007, Paper no. 67080D, doi: 10.1117/12.736368.
[22] Y. Ma, P. Zhou, X. Wang, K. Han, H. Ma, X. Xu, L. Si, Z. Liu, and Y. Zhao, "Coherent beam combination of two thulium-doped fiber laser beams with the multi-ditheringtechnique," *Opt. Laser Technol.*, vol. 43, no. 3, pp. 721–724, Apr. 2011, doi: 10.1016/j.optlastec.2010.09.015.
[23] Y. Ma, P. Zhou, K. Zhang, X. Wang, H. Ma, X. Xu, L. Si, Z. Liu, and Y. Zhao, "A coherent beam combination system based on double PZT phase modulators," *Appl. Phys. B, Lasers Opt.*, vol. 107, no. 3, pp. 765–769, Jun. 2012, doi: 10.1007/s00340-012-4994-9.
[24] C. Geng, W. Luo, Y. Tan, H. Liu, J. Mu, and X. Li, "Experimental demonstration of using divergence cost-function in SPGD algorithm for coherent beam combining with tip/tilt control," *Opt. Exp.*, vol. 21, no. 21, p. 25045, Oct. 2013, doi: 10.1364/OE.21.025045.
[25] X. Wang, Y. Ma, P. Zhou, B. He, H. Xiao, Y. Xue, C. Liu, Z. Li, X. Xu, J. Zhou, Z. Liu, and Y. Zhao, "Coherent beam combining of 137 W 2 × 2 fiber amplifier array," *Opt. Commun.*, vol. 284, no. 8, pp. 2198–2201, Apr. 2011, doi: 10.1016/j.optcom.2010.12.090.
[26] P. Zhou, Z. Liu, X. Wang, Y. Ma, H. Ma, X. Xu, and S. Guo, "Coherent beam combining of fiber amplifiers using stochastic parallel gradient descent algorithm and its application," *IEEE J. Sel. Topics Quantum Electron.*, vol. 15, no. 2, pp. 248–256, Mar./Apr. 2009, doi: 10.1109/JSTQE.2008.2010231.
[27] P. Bourdon, H. Jacqmin, B. Augère, A. Durécu, D. Goular, B. Rouzè, R. Domel, D. Fleury, C. Planchat, and L. Lombard, "Target-in-the-loop coherent combining of 7 fiber lasers: First results," in *Proc. OPTRO*, Paris, France, Jan. 2020, pp. 1–6.
[28] H. K. Ahn, S. W. Park, and H. J. Kong, "PZT-modulated coherent four-beam combination system with high-control bandwidth by using modified multi-dithering theory," *Appl. Phys. B, Lasers Opt.*, vol. 118, no. 1, pp. 7–10, Jan. 2015, doi: 10.1007/s00340-014-5947-2.
[29] Y. Ma, X. Wang, P. Zhou, B. He, H. Xiao, Y. Xue, C. Liu, Z. Li, X. Xu, J. Zhou, L. Si, Z. Liu, and Y. Zhao, "Coherent beam combination of 137 W fiber amplifier array using single frequency dithering technique," *Opt. Lasers Eng.*, vol. 49, no. 8, pp. 1089–1092, Aug. 2011, doi: 10.1016/j.optlaseng.2011.03.001.
[30] M. A. Vorontsov and S. L. Lachinova, "Laser beam projection with adaptive array of fiber collimators i basic considerations for analysis," *J. Opt. Soc. Amer. A, Opt. Image Sci.*, vol. 25, no. 8, p. 1949, Aug. 2008, doi: 10.1364/JOSAA.25.001949.
[31] X. Fan, J. Liu, J. Liu, and J. Wu, "Coherent combining of a seven-element hexagonal fiber array," *Opt. Laser Technol.*, vol. 42, no. 2, pp. 274–279, Mar. 2010, doi: 10.1016/j.optlastec.2009.07.004.
[32] T. M. Shay, "Theory of electronically phased coherent beam combination without a reference beam," *Opt. Exp.*, vol. 14, no. 25, p. 12188, 2006, doi: 10.1364/OE.14.012188.

PAWEL R. KACZMAREK received the M.S. degree in optoelectronic engineering and the Ph.D. degree in telecommunications from the Wroclaw University of Science and Technology (WrUT), Wroclaw, Poland, in 2000 and 2005, respectively.

Since 2005, he has been with Lasers, Fibers Electronics Group, WrUT, as an Assistant Professor. In 2006, he spent a month Short Term Scientific Mission in the frame of COST291 "Toward Digital Optical Networks" action as a Research Assistant with CNIT, Pisa, Italy. He has authored or coauthored more than 70 scientific publications and 25 in peer-reviewed journals. His main research interests include optical fiber interferometry supported by optical amplifiers, high-power fiber amplifiers and lasers, coherent beam combining, pulsed fiber lasers, electronics, and signal processing for fiber lasers.

ALEKSANDER GLUSZEK received the B.S. and M.S. degrees in electrical engineering from the Wroclaw University of Science and Technology, Wroclaw, Poland, in 2013 and 2015, respectively, where he is currently pursuing the Ph.D. degree in automation, electronic and electrical engineering. From 2015 to 2016, he was a Research Assistant with Rice University Laser Science Group, Houston, TX, USA. In 2017, he was a Research Assistant with the Department of Electrical and Computer Engineering, Princeton University, USA. His research interests include the development of fiber comb lasers, precision and low noise electronics, micromechanics, 3D printing, and digital signal processing and its application in laser spectroscopy. His awards and honors include the Scholarship of the Minister of Science and Higher Education for outstanding achievements, in 2018.

ARKADIUSZ HUDZIKOWSKI was born in Tychy, Poland, in 1990. He received the B.S. degree in measuring equipment, the M.S. degree in advanced applied electronics, and the Ph.D. degree in automation, electronic and electrical engineering from the Wroclaw University of Science and Technology, Poland, in 2013, 2015, and 2022, respectively.

From 2015 to 2016, he was a Research Assistant with the Laser Science Group, Rice University, Houston, USA. In 2017, he was a Research Assistant with the Department of Electrical and Computer Engineering, Princeton University, USA. His research interests include the development of precision and low noise electronics instrumentation, laser spectroscopy, and laser ultrashort pulse compression.

Dr. Hudzikowski's awards and honors include the Scholarship of the Minister of Science and Higher Education for outstanding achievements, in 2018.